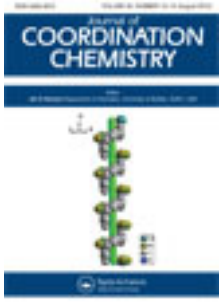

Journal of Coordination Chemistry
Publication details, including instructions for authors and subscription information:
http://www.tandfonline.com/loi/gcoo20

Synthesis, crystal structure, and magnetism of [Mn(hfac)$_2$NIT(Ph-m-OPh)]

Xiang Yang Qin [a], Gang Xiong [b], DaiZheng Liao [c], Yue Ma [c], Peng Gao [a], Xiao Li Sun [a] & Peng Liu [a]

[a] Department of Chemistry, School of Pharmacy, Fourth Military Medical University, Xi'an 710032, PR China

[b] Department of Chemistry, College of Science, Tianjin University, Tianjin 300072, PR China

[c] Department of Chemistry, Nankai University, Tianjin 300071, PR China

Accepted author version posted online: 06 Jun 2012.Published online: 20 Jun 2012.

To cite this article: Xiang Yang Qin, Gang Xiong, DaiZheng Liao, Yue Ma, Peng Gao, Xiao Li Sun & Peng Liu (2012) Synthesis, crystal structure, and magnetism of [Mn(hfac)$_2$NIT(Ph-m-OPh)], Journal of Coordination Chemistry, 65:15, 2683-2691, DOI: 10.1080/00958972.2012.699633

To link to this article: http://dx.doi.org/10.1080/00958972.2012.699633

Journal of Coordination Chemistry
Vol. 65, No. 15, 10 August 2012, 2683–2691

Synthesis, crystal structure, and magnetism of [Mn(hfac)$_2$NIT(Ph-*m*-OPh)]

XIANG YANG QIN†¶, GANG XIONG‡¶, DAIZHENG LIAO§, YUE MA§, PENG GAO†, XIAO LI SUN† and PENG LIU*†

†Department of Chemistry, School of Pharmacy, Fourth Military Medical University, Xi'an 710032, PR China
‡Department of Chemistry, College of Science, Tianjin University, Tianjin 300072, PR China
§Department of Chemistry, Nankai University, Tianjin 300071, PR China

(*Received 15 October 2011; in final form 24 April 2012*)

A new complex [Mn(hfac)$_2$NIT(Ph-*m*-OPh)] has been synthesized and structurally characterized by X-ray diffraction. It crystallizes in the monoclinic space group *P2(1)/c*. The structure consists of a 1-D chain with Mn(II) bridged by NIT(Ph-*m*-OPh). The manganese(II) is in a distorted octahedral environment formed by one oxygen from NIT(Ph-*m*-OPh) and three atoms from hexafluoro acetylacetone (hfac) in the equatorial plane and two oxygens from hfac and the other NIT(Ph-*m*-OPh) in the axial position. The units of [Mn(hfac)$_2$NIT(Ph-*m*-OPh)] are connected as a 1-D chain by Mn(II) and oxygen of N–O in bridging NIT(Ph-*m*-OPh) along the *b*-axis. The 2-D layer in the *ab* plane is formed *via* hydrogen interactions to connect neighboring chains. The complex exhibits intramolecular antiferromagnetic interactions between Mn(II) and NIT(Ph-*m*-OPh).

Keywords: Crystal structure; Nitronyl nitroxide; Manganese(II) complex; Antiferromagnetic interactions

1. Introduction

Design and synthesis of molecule-based magnetic materials is a major subject of materials science [1]. Molecular magnets constructed by magnetic metal ions and nitronyl nitroxides are attractive due to nitronyl nitroxides acting as magnetic couplers [2]. Derivatives of nitronyl nitroxides are of great importance in exploring molecular-based magnetic materials. NITR, a nitronyl nitroxide, was utilized to coordinate with Mn(hfac)$_2$ (hfac = 1,1,1,5,5,5-hexafluoropentane-2,4-dionate) in synthesizing magnetic material [3]. However, NITRs are poor electron-donor ligands with limited coordination ability. The radical NIT(Ph-*m*-OPh) was a promising candidate because it possesses an electron-rich phenoxy group (figure 1) [4]. Alternation of such

*Corresponding author. Email: pengliu@fmmu.edu.cn
¶Xiang Yang Qin and Gang Xiong are co-first authors.

ISSN 0095-8972 print/ISSN 1029-0389 online
http://dx.doi.org/10.1080/00958972.2012.699633

NIT(Ph-*m*-OPh):

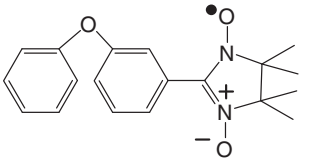

Figure 1. The chemical structure of NIT(Ph-*m*-OPh).

electron-rich groups with the electron-poor rings occurs when hfac coordinating to a metal center favors stacking interactions along the chain, thus stabilizing the polymeric compound [4]. By taking advantage of the abilities of NIT(Ph-*m*-OPh) and hfac to coordinate to transition metals, we have synthesized the metal–radical complex, [Mn(hfac)$_2$NIT(Ph-*m*-OPh)].

Here, we report the synthesis and structure of the radical NIT(Ph-*m*-OPh) and that of the manganese complex; the magnetic property of the complex is also discussed.

2. Experimental

2.1. *General*

All starting materials were analytical grade. Elemental analyses for carbon, hydrogen, and nitrogen were carried out on a Model 240 Perkin–Elmer elemental analyzer. The infrared spectrum was taken on a Shimadzu IR spectrophotometer model 408 from 4000–600 cm^{-1} using KBr pellets. Magnetic susceptibility of the crystalline sample was carried out from 2–300 K on a SQUID-XL-7 magnetometer at 2000 G. Diamagnetic corrections were made with Pascal's constants for all constituent atoms.

2.2. *Preparation of NIT(Ph-m-OPh)*

3-(1-Phenoxybenzene)-4,4,5,5-tetramethylimidazoline-1-oxyl-3-oxide was prepared by the literature method [5, 6]. NIT(Ph-*m*-OPh) was crystallized from ethyl acetate/petroleum (4 : 1) as dark blue needles.

2.3. *Preparation of [Mn(hfac)$_2$NIT(Ph-m-OPh)]*

Mn(hfac)$_2 \cdot 2H_2O$ (26 mg, 0.05 mmol) was dissolved in boiling dry *n*-heptane (40 mL). The solution was left to boil for 1 h, cooled to 65°C, and then a solution of NIT(Ph-*m*-OPh) (16 mg, 0.05 mmol) in dry CH_2Cl_2 (20 mL) was slowly added while stirring. The mixture was stirred for 1 h at 65°C. The final solution was cooled to room temperature and filtered. The green filtrate was allowed to stand at −10°C for 15 days. Dark-blue crystals were obtained (35.3 mg, 89.2%). Anal. Calcd for [Mn(hfac)$_2$NIT(Ph-*m*-OPh)]: C, 43.84; H, 2.92; N, 3.53. Found (%): C, 43.67; H, 2.88; N, 3.56.

Table 1. Crystal data and structure refinement for NIT(Ph-*m*-OPh) and [Mn(hfac)$_2$NIT(Ph-*m*-OPh)].

Compound	NIT(Ph-*m*-OPh)	[Mn(hfac)$_2$NIT(Ph-*m*-OPh)]
Empirical formula	$C_{19}H_{21}N_2O_3$	$C_{29}H_{23}F_{12}MnN_2O_7$
Formula weight	325.38	794.43
Crystal system	Monoclinic	Monoclinic
Space group	*P2(1)/n*	*P2(1)/c*
a	6.0247(10)	11.553(2)
b	11.7151(19)	14.186(3)
c	24.080(4)	21.544(4)
α	90	90
β	94.004(3)	104.93(3)
γ	90	90
Volume (Å^3), *Z*	1695.4(3), 4	3411.7(11), 4
Calculated density (g cm^{-3})	1.275	1.547
Absorption coefficient (mm^{-1})	0.087	0.499
F(000)	692	1600
Crystal size (mm^3)	0.38 × 0.28 × 0.18	0.20 × 0.20 × 0.18
θ range for data collection (°)	1.70–25.10	3.00–25.01
Limiting indices	$-6 \le h \le 7$; $-13 \le k \le 13$; $-24 \le l \le 28$	$-13 \le h \le 13$; $-16 \le k \le 16$; $-25 \le l \le 25$
Reflections collected	8361	27,366
Independent reflection	3007 [*R*(int) = 0.0425]	6011 [*R*(int) = 0.0624]
Goodness-of-fit on F^2	1.063	1.131
Final *R* indices [$I > 2\sigma(I)$]	$R_1^a = 0.0503$, $wR_2^b = 0.1208$	$R_1^a = 0.0646$, $wR_2^b = 0.1459$
R indices (all data)	$R_1 = 0.0916$, $wR_2 = 0.1486$	$R_1 = 0.0882$, $wR_2 = 0.1581$

[a] $R_1 = \Sigma||F_o| - |F_c||/\sum|F_o|$; [b] $wR_2 = \{\Sigma[w(F_o^2 - F_c^2)]/\Sigma[w(F_o^2)]\}^{1/2}$, $w = 1/[\sigma^2(F_o^2) + (0.0900P)^2 + 0.0000P]$ where $P = (F_o^2 + 2F_c^2)/3$.

2.4. *X-ray crystallographic determination*

A suitable single crystal was put on a Bruker Smart 1000 CCD X-ray diffractometer and collection of crystallographic data was carried out using graphite-monochromated Mo-Kα radiation (0.71073 Å) at 298 K in the ω–2θ scan mode. An empirical absorption correction was applied to the data using SADABS. The structures were solved by direct methods and refined by full-matrix least-squares on F^2 using the SHELXTL crystallographic software package [7]. All non-H atoms were refined anisotropically. Hydrogens were placed in calculated positions and refined by using a riding mode with Uiso(H) = 1.5 Ueq(C) for methyl and 1.2 Ueq(C) for the others. In order to retain an acceptable displacement parameter in [Mn(hfac)$_2$NIT(Ph-*m*-OPh)], fluorines have been treated using part instruction. Crystallographic data and selected bond lengths and angles for NIT(Ph-*m*-OPh) and [Mn(hfac)$_2$NIT(Ph-*m*-OPh)] are listed in tables 1 and 2, respectively.

3. Results and discussion

3.1. *Description of NIT(Ph-m-OPh) structure*

A sketch of NIT(Ph-*m*-OPh) is shown in figure 2. The radical NIT(Ph-*m*-OPh) crystallizes in the monoclinic *P2(1)/c* space group. The dihedral angle between the phenyl ring (C1–C6) and phenyl ring (C7–C12) bridged by O1 is 59.37°. The torsion NCCN is −19.432°, which suggests that the imidazole ring is twisted. The two N–O

Table 2. Selected bond distances (Å) and angles (°).

NIT(Ph-*m*-OPh)			
O(1)–C(7)	1.390(3)	O(1)–C(6)	1.391(3)
O(2)–N(1)	1.284(2)	O(3)–N(2)	1.280(2)
N(1)–C(13)	1.348(3)	N(1)–C(14)	1.494(3)
N(2)–C(13)	1.348(3)	N(2)–C(17)	1.513(3)
C(7)–O(1)–C(6)	120.5(2)	O(2)–N(1)–C(13)	126.13(19)
O(2)–N(1)–C(14)	120.53(17)	C(13)–N(1)–C(14)	112.91(18)
O(3)–N(2)–C(13)	126.29(19)	O(3)–N(2)–C(17)	120.63(17)
C(13)–N(2)–C(17)	112.50(19)	N(1)–C(13)–N(2)	108.1(2)
N(1)–C(13)–C(11)	125.9(2)	N(2)–C(13)–C(11)	125.9(2)
N(1)–C(14)–C(16)	108.97(19)	N(1)–C(14)–C(15)	106.17(18)
[Mn(hfac)$_2$NIT(Ph-*m*-OPh)]			
Mn(1)–O(6)	2.131(3)	Mn(1)–O(2)#1	2.142(3)
Mn(1)–O(1)	2.142(3)	Mn(1)–O(5)	2.155(3)
Mn(1)–O(4)	2.164(3)	Mn(1)–O(7)	2.165(3)
C(1)–N(1)	1.326(5)	C(1)–N(2)	1.341(4)
N(1)–O(1)	1.288(4)	N(2)–O(2)	1.287(4)
O(2)–Mn(1)#2	2.142(3)	O(6)–Mn(1)–O(2)#1	101.37(11)
O(6)–Mn(1)–O(1)	87.95(11)	O(2)#1–Mn(1)–O(1)	88.08(10)
O(6)–Mn(1)–O(5)	156.34(13)	O(2)#1–Mn(1)–O(5)	94.91(11)
O(1)–Mn(1)–O(5)	109.82(11)	O(6)–Mn(1)–O(4)	84.75(13)
O(2)#1–Mn(1)–O(4)	173.71(12)	O(1)–Mn(1)–O(4)	90
O(5)–Mn(1)–O(4)	79.69(12)	O(6)–Mn(1)–O(7)	81.47(11)
O(1)–Mn(1)–O(7)	168.40(11)	O(5)–Mn(1)–O(7)	81.67(12)
O(4)–Mn(1)–O(7)	93.00(12)	O(1)–N(1)–C(1)	125.7(3)
O(1)–N(1)–C(2)	122.1(3)	C(1)–N(1)–C(2)	111.8(3)
O(2)–N(2)–C(1)	126.0(3)	O(2)–N(2)–C(5)	121.4(3)
C(1)–N(2)–C(5)	111.8(3)	N(1)–O(1)–Mn(1)	126.8(2)
N(2)–O(2)–Mn(1)#2	123.7(2)	C(14)–O(3)–C(12)	117.4(3)

Symmetry transformations used to generate equivalent atoms: #1 $-x+1$, $y+1/2$, $-z+1/2$; #2 $-x+1$, $y-1/2$, $-z+1/2$.

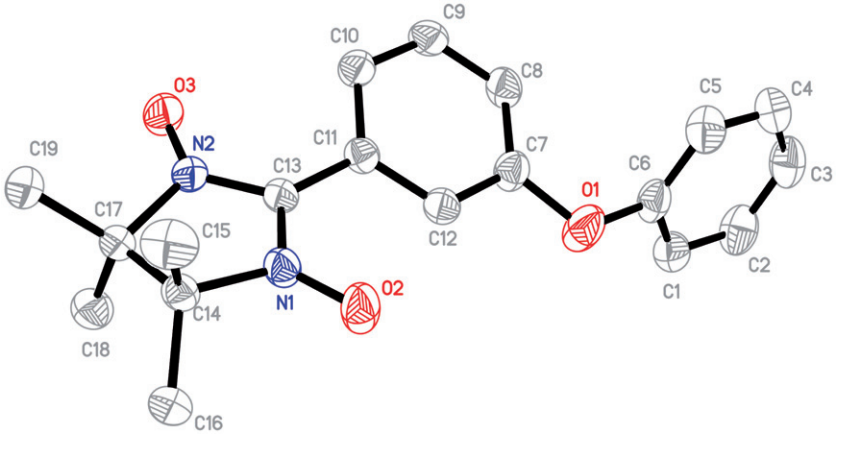

Figure 2. The structure of NIT(Ph-*m*-OPh) with labeling scheme and ellipsoids drawn at the 30% probability level.

bond lengths are 1.284(2) and 1.280(2) Å. Formation of strong intramolecular hydrogen bonds [C_{sp2}–H···O] between a hydrogen at the 2-position of the phenyl group and oxygen (O2, O3) of the NO groups of the same molecule and intermolecular hydrogen bonding [C_{sp3}–H···O] between the methyl hydrogen attached to the imidazolyl ring of

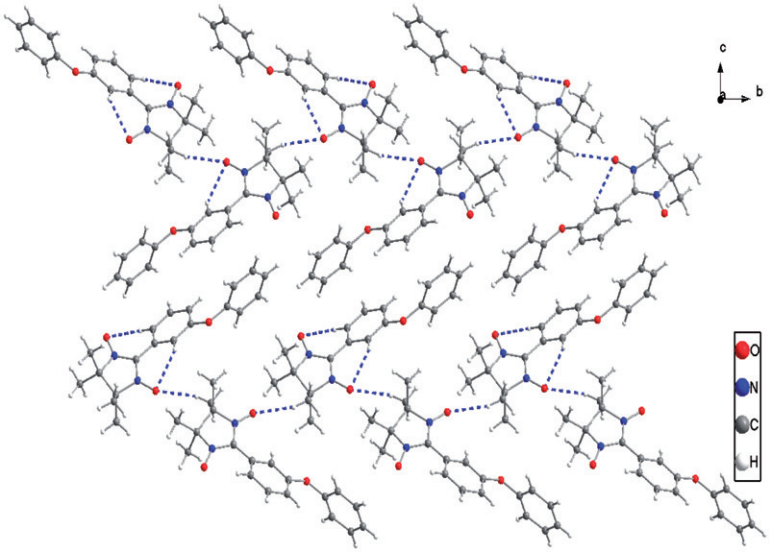

Figure 3. 1-D chain *via* hydrogen bond interaction in NIT(Ph-*m*-OPh).

Table 3. Intermolecular hydrogen bonds of NIT(Ph-*m*-OPh) and [Mn(hfac)$_2$NIT(Ph-*m*-OPh)] (Å, °).

	D–H···A	D–H	H···A	D···A	D–H···A
NIT(Ph-*m*-OPh)	C(16)–H(16B)···O(2)#1	0.96	2.49	3.4011	158
	C(19)–H(19B)···O(2)#2	0.96	2.52	3.3993	153
[Mn(hfac)$_2$NIT(Ph-*m*-OPh)]	C(7)–H(7B)···F(12)#1	0.96	2.48	3.2640	139

Symmetry transformations used to generate equivalent atoms: For NIT(Ph-*m*-OPh) #1 $-x+1$, $y-0.5$, $1.5-z$; #2 $-x+2$, $y-0.5$, $3/2-z$. For [Mn(hfac)$_2$NIT(Ph-*m*-OPh)] #1 $1-x$, $-1/2+y$, $1/2-z$.

one molecule and the oxygen associated with the longer N–O group of a neighboring molecule allows for an infinite supermolecular chain (figure 3 and table 3).

3.2. *Description of [Mn(hfac)$_2$NIT(Ph-m-OPh)] structure*

A sketch of [Mn(hfac)$_2$NIT(Ph-*m*-OPh)] is shown in figure 4. The manganese(II) is six-coordinate in a distorted octahedral MnO_6 environment. The equatorial plane is formed by O4, O5, and O6 from hfac, and O2A from NIT(Ph-*m*-OPh). The Mn–O bond lengths in the plane are 2.131(3), 2.142(3), 2.155(3), and 2.164(3) Å for Mn(1)–O(6), Mn1–O2A, Mn1–O5, and Mn1–O4, respectively, in the normal range [8]. The axial positions are occupied by two oxygens, one from hfac and one from NIT(Ph-*m*-OPh).The axial Mn–O bond lengths are 2.142(3) and 2.165(3) Å for Mn1–O1 and Mn1–O7, respectively. The bond angle of O1–Mn1–O7 is 168.40(11). The units of [Mn(hfac)$_2$NIT(Ph-*m*-OPh)] are connected as a 1-D chain by manganese(II) and oxygen of the N–O bond in the bridging NIT(Ph-*m*-OPh) along the *b*-axis.

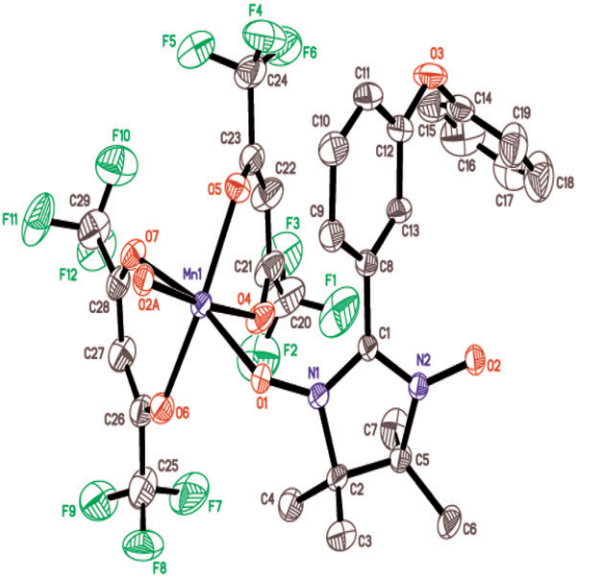

Figure 4. The structure of [Mn(hfac)$_2$NIT(Ph-*m*-OPh)] with labeling scheme and ellipsoids drawn at the 30% probability level.

Additionally, the 2-D layer in the *ab* plane is formed *via* hydrogen bonds (C_7–$H_{7b}\cdots F_{12}$) and connects neighboring chains (figure 5 and table 3).

3.3. *Spectroscopic properties*

The infrared spectrum of [Mn(hfac)$_2$NIT(Ph-*m*-OPh)] displays hexafluoro acetylacetone coordinated with manganese(II) by enol. Bands at 1650 and 1502 cm^{-1} are characteristic bands of $\nu_{C\cdots O}$ and $\nu_{C\cdots C}$. The weak peak at 1338 cm^{-1} is assigned to the stretching frequency of N–O, which is lower than the 1363 cm^{-1} value of ν(N–O) of free NIT(Ph-*m*-OPh), indicating that the N–O of NIT(Ph-*m*-OPh) is coordinated to Mn(II), consistent with reported findings [3].

3.4. *Magnetic properties*

The magnetic susceptibilities, χ_m, of the complex were measured from 2–300 K at 2000 G; figure 6 shows the plot of $\chi_m T$ and χ_m *versus* T. The $\chi_m T$ value of the complex is 5.9 cm^3 mol^{-1} K at 300 K, slightly larger than the calculated value of 4.75 cm^3 mol$^{-1}\cdot$ K for a non-coupled system ($g = 2.0$). Upon cooling, the $\chi_m T$ increased to a maximum of 65.8 cm^3 mol^{-1} K at 12 K and then quickly decreased. The maximum values are much larger than that of $S = 2$ (3.0 cm^3 mol^{-1} K) due to an antiferromagnetically correlated unit for [Mn(hfac)$_2$NIT(Ph-*m*-OPh)]. This magnetic behavior indicates that ferrimagnetic interaction with alternating $S = 5/2$ and $S = 1/2$ spins is operative infinitely along the chain structures [8–10].

We analyzed the data on the basis of the equation (1) [1a], derived from the Hamiltonians $H = -J\sum S_{Bi}\cdot[(1+\alpha)S_{Ai} + (1-\alpha)S_{Ai+1}]$. We introduced zJ', the

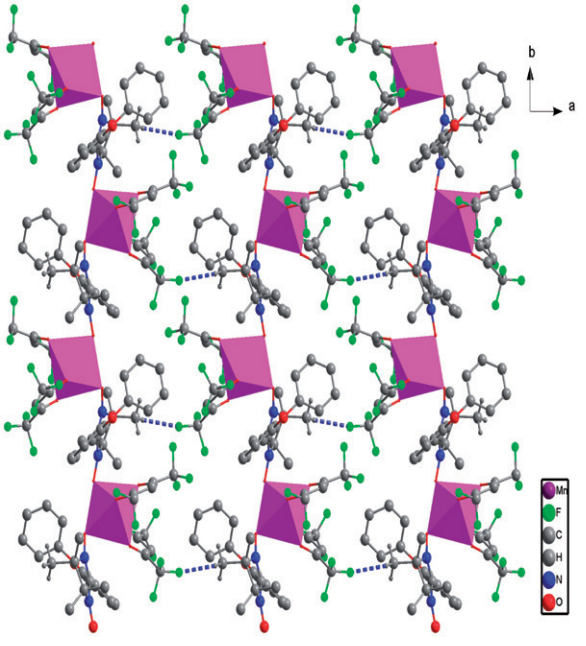

Figure 5. 2-D layer *via* hydrogen bond interaction in [Mn(hfac)$_2$NIT(Ph-*m*-OPh)].

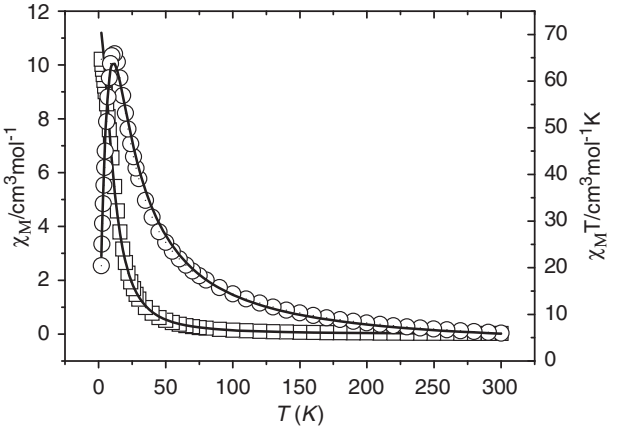

Figure 6. Temperature dependence of $\chi_m T$ (○) nd χ_m (□) measured at 2000 Oe for [Mn(hfac)$_2$NIT(Ph-*m*-OPh)]; the solid line shows the best fit to the data.

interaction between chains, using molecular field approximation. The definition of P, Q, and R as a function of J/kT is described [1a], s is treated as a quantum spin, and the g-value ($g(5/2)$, $g(1/2)$) is fixed to 2.00. The other constants, N, k, and β, are defined as their usual meanings.

$$\chi = \frac{N\beta^2}{3kT}\frac{g^2[s(s+1)(1-P)+2QR]+2gG(Q+R)+G^2(1+P)}{1-P} \quad (1)$$

Table 4. Selected magnetic parameters (J) for Mn(II) and NITR nitroxide radical compounds.

R	J (cm^{-1})	g	Mn–O–N (°)	References
PhOMe	−344	2.0	131.14, 127.37	[13]
i-Pr	−329.8	2.0	134.72	[3]
Et	−260	2.0	137.15, 127.14	[14]
Bzald	−225	2.0	122.00	[15]
Ph-*m*-OPh	−220	2.0	123.69, 126.82	This work
Me	−216.7	2.0	–	[3]
Ph	−208.2	2.0	–	[3]
phIm	−200.38	2.0	124.92	[11]
PhBr	−129.4	2.02	124.18, 123.60	[9]
phPyrim	− 87.61	2.0	133.04	[16]
$PhNEt_2$	−34.2	2.0	128.93, 125.49	[10]

Bzald = 4-benzaldehyde, phIm = 4-(1-imidazole)phenyl], phPyrim = 4-(5-pyrimidyl)phenyl; – represents no crystal data.

The best-fit parameters are $J_1 = J_2 = -220\,cm^{-1}$, $zJ' = -0.09\,cm^{-1}$ with $R_{chi} = 0.0054$, $R_{mu} = 0.000554$, J_1 and J_2 represents the Mn(II) – NITPh-*m*-OPh – Mn(II) interacting. The negative J and small zJ' indicates the existence of antiferromagnetic interaction of intrachain and weak antiferromagnetic interaction between Mn(II) – Rad chains, while the strong antiferromagnetic interaction is thought to result from smaller angle of Mn–O–N (123.69° and 126.82°), which lead to effective overlap of *p*-SOMO of the nitroxide and the d-orbitals on Mn(II) [11, 12, 16]. From table 4, the angles of Mn–O–N in the Mn-radical complex with strong antiferromagnetic interaction fall in the range 122–137.15°; the small angles benefit overlap of orbitals, which are capable of overcoming ferromagnetic interaction [9]. The inductive effect of phenoxy, which enhances the electron density on the radical, can also account for the strong antiferromagnetic interaction.

4. Conclusion

[$Mn(hfac)_2$NIT(Ph-*m*-OPh)] is a further example of a 1-D metal-nitronyl nitroxide radical complex. Magnetic coupling between Mn(II) and NIT(Ph-*m*-OPh) shows strong antiferromagnetic interactions. The radical of NIT(Ph-*m*-OPh) is a promising ligand for development of strongly correlated 1-D ferrimagnetic systems, as demonstrated by [$Mn(hfac)_2$NIT(Ph-*m*-OPh)].

Supplementary material

Crystallographic data for the structural analysis have been deposited with the Cambridge Crystallographic Data Centre, CCDC No. 724596 and 775688. Copies of this information can be obtained free of charge from The Director, CCDC, 12 Union Road, Cambridge, CB2 1EZ, UK (Fax: +44-1223-336-033; E-mail: deposit@ccdc.cam.ac.uk or https://www.ccdc.cam.ac.uk/services/structure_deposit/).

Acknowledgments

We thank Prof. Hiroshi Sakiyama (Yamagata University, Japan) for helping us to fit the magnetochemical data. Besides, this work was supported by the National Science Foundation of China (No. 21172261).

References

[1] (a) O. Kahn. *Molecular Magnetism*, VCH, New York (1993); (b) J. Mrozinńsky. *Coord. Chem. Rev.*, **249**, 2534 (2005).
[2] (a) K.E. Vostrikova. *Coord. Chem. Rev.*, **252**, 1409 (2008); (b) S. Miller, M. Drillon. *Magnetism Molecules to Materials: Models and Experiments*, Wiley-VCH, Weinheim (2002).
[3] A. Caneschi, D. Gatteschi, R. Sessoli. *Inorg. Chem.*, **27**, 1756 (1988).
[4] L. Bogani, C. Sangregorio, R. Sessoli, D. Gatteschi. *Angew. Chem., Int. Ed.*, **44**, 5817 (2005).
[5] E.F. Ullman, J.H. Osiecki, D.G.B. Boocock, R. Darcy. *J. Am. Chem. Soc.*, **94**, 7049 (1974).
[6] E.F. Ullman, L. Call, J.H. Osiecki. *J. Org. Chem.*, **35**, 3623 (1970).
[7] G.M. Sheldrick. *SHELX 97, PC Version*, University of Göttingen, Germany (1997).
[8] T. Ise, T. Ishida, D. Hashizume, F. Iwasaki, T. Nogami. *Inorg. Chem.*, **42**, 6106 (2003).
[9] C.-X. Zhang, X.-Y. Zhao, N.-N. Sun, Y.-L. Guo, Y.Y. Zhang. *Inorg. Chim. Acta*, **367**, 135 (2011).
[10] Z.-L. Liu, Q.-H. Zhao, S.-Q. Li, D.-Z. Liao, Z.-H. Jiang, S.-P. Yan. *Inorg. Chem. Commun.*, **4**, 322 (2001).
[11] R.-N. Liu, L.-C. Li, X.-Y. Xing, D.-Z. Liao. *Inorg. Chim. Acta*, **362**, 2253 (2009).
[12] D. Luneau, P. Rey, J. Laugier, P. Fries, A. Caneschi, D. Gatteschi, R. Sessoli. *J. Am. Chem. Soc.*, **113**, 1245 (1991).
[13] A. Caneschi, D. Gatteschi, P. Rey, R. Sessolit. *Inorg. Chem.*, **30**, 3936 (1991).
[14] A. Caneschi, D. Gatteschi, J.P. Renard, P. Rey, R. Sessoli. *Inorg. Chem.*, **28**, 3314 (1989).
[15] A. Caneschi, D. Gatteschi, R. Sessoli. *Inorg. Chem.*, **32**, 4612 (1993).
[16] J.-Y. Zhang, C.-M. Liu, D.-Q. Zhang, S. Gao, D.-B. Zhu. *Inorg. Chim. Acta*, **360**, 3553 (2007).